Self-organized 2D nanopatterns after low-coverage Ga adsorption on Si (1 1 1)

2005 New J. Phys. 7 193

(http://iopscience.iop.org/1367-2630/7/1/193)

New Journal of Physics
The open-access journal for physics

Self-organized 2D nanopatterns after low-coverage Ga adsorption on Si (1 1 1)

Thomas Schmidt[1,3], **Subhashis Gangopadhyay**[1], **Jan Ingo Flege**[1], **Torben Clausen**[1], **Andrea Locatelli**[2], **Stefan Heun**[2,4] **and Jens Falta**[1]

[1] Institute of Solid State Physics, University of Bremen, Otto-Hahn-Allee 1, 28 359 Bremen, Germany
[2] ELETTRA Synchrotron Light Source, Strada Statale 14, 34012 Basovizza, Italy
E-mail: tschmidt@ifp.uni-bremen.de

New Journal of Physics **7** (2005) 193
Received 2 June 2005
Published 13 September 2005
Online at http://www.njp.org/
doi:10.1088/1367-2630/7/1/193

Abstract. The evolution of the Si(1 1 1) surface after submonolayer deposition of Ga has been observed *in situ* by low-energy electron microscopy and scanning tunnelling microscopy. A phase separation of Ga-terminated $\sqrt{3} \times \sqrt{3}$-R 30° reconstructed areas and bare Si(1 1 1)-7 × 7 regions leads to the formation of a two-dimensional nanopattern. The shape of this pattern can be controlled by the choice of the surface miscut direction, which is explained in terms of the anisotropy of the domain boundary line energy and a high kink-formation energy. A general scheme for the nanopattern formation, based on intrinsic properties of the Si(1 1 1) surface, is presented. Experiments performed with In instead of Ga support this scheme.

[3] Author to whom any correspondence should be addressed.
[4] Present address: TASC-INFM Laboratory, Area di Ricerca, 34012 Basovizza, Italy.

PII: S1367-2630(05)00982-1

Contents

1. Introduction

The nanoscale patterning of semiconductor surfaces has become an important issue in surface science and technology. Changes of the surface properties after adsorbate-induced nanopattern formation can enable selective growth of nanometre scale structures such as nanowires or nanodots. Different routes have been taken towards surface patterning: single-atom manipulation [1, 2], electron or ion beam lithography [3, 4] and self-assembly [5, 6] of surface patterns. The latter is especially promising with respect to technological applications, because it opens the gate towards the massively parallel fabrication of device structures.

The Ga/Si(1 1 1) system is of special interest, because it has already been demonstrated that nanoscale pattern formation can be achieved and, moreover, subsequent selective growth and alignment of three-dimensional (3D) germanium nanoislands is possible [7]. For this specific adsorbate system, it has been reported that the miscut direction can affect the shape of the Ga : Si(1 1 1)-$\sqrt{3} \times \sqrt{3}$-R 30° domains [8] after room temperature saturation and (partial) thermal redesorption of gallium. In the following, we will not only show how the nanopattern shape can be controlled during Ga deposition, but we will also elucidate the mechanism responsible for this type of nanopattern formation.

2. Experimental

The experiments were carried out in two different ultra-high vacuum systems. One system is equipped with a variable-temperature scanning tunnelling microscope (Omicron VT-STM). The other system is the spectroscopic photoemission and low-energy electron microscope (SPELEEM) at the undulator beamline 1.2 at ELETTRA [9, 10]. After degassing the Si(1 1 1) substrates for at least 12 h at 600 °C, a clean 7 × 7 surface reconstruction was prepared by 2 or 3 short flashes to 1200 °C for up to 30 s. Ga was evaporated from an effusion cell heated by electron bombardment. For the STM experiments, Ga was deposited at room temperature, and the sample temperature was then increased during the STM measurements. For the LEEM studies, highly oriented Si wafer pieces with an absolute miscut angle of about 0.02° were used. Ga was deposited during imaging in the LEEM, at a sample temperature close to the Ga redesorption

threshold (≈650 °C), i.e. very close to thermodynamic equilibrium conditions. The values of the absolute Ga coverages given in the following have been determined from the area fractions of the Ga-$\sqrt{3} \times \sqrt{3}$-R 30° structure appearing in the LEEM and STM images, which is known to have a local coverage of 1/3 ML (1 ML = 7.83×10^{14} atoms cm^{-2}).

3. Results and discussion

3.1. LEEM results for different miscut directions

The topography of a Si(1 1 1) surface with a miscut orientation towards [1 1 $\bar{2}$] and its evolution during Ga deposition at about 650 °C is shown in figure 1. For the electron energy chosen here, the Ga : Si(1 1 1)-$\sqrt{3} \times \sqrt{3}$-R 30° reconstruction (henceforth simply referred to as $\sqrt{3}$) appears dark, whereas the 7 × 7 superstructure appears bright. (This was confirmed by dark-field images not shown here.) The nucleation of the $\sqrt{3}$ structure takes place both at initial domain boundaries (IDBs) of the 7 × 7 reconstruction and on the lower terrace side of the step edges. At the beginning, the $\sqrt{3}$ domains are composed of equilateral triangles, with the outward normal of the edges pointing along ⟨$\bar{1}$ $\bar{1}$ 2⟩. As can be seen from the images, the $\sqrt{3}$ areas grow with comparable speed at the step edges and at the IDBs. It is also obvious that at the step edges the growth proceeds only towards the lower terrace, whereas at the IDBs, the $\sqrt{3}$ structure develops towards both the [1 $\bar{1}$ 0] and the [$\bar{1}$ 1 0], direction. As soon as the $\sqrt{3}$ reconstruction dominates the surface topology, the remaining patches of the 7 × 7 form equilateral triangles with the outward normal of the edges pointing along ⟨1 1 $\bar{2}$⟩.

A different surface topology is observed, however, if the miscut points to the opposite direction: figure 2 shows the evolution for the same preparation conditions as in figure 1, but for a surface with a miscut along [$\bar{1}$ $\bar{1}$ 2]. Again, the formation of a nanopattern of $\sqrt{3}$ domains is observed. The $\sqrt{3}$ structure again grows from step edges (on lower terraces) and IDBs (both towards [$\bar{1}$ 1 0] and [1 $\bar{1}$ 0] direction), but the growth rate at step edges is much smaller than at the IDBs, and the triangular shape of the domains is less pronounced. This leads to the formation of a rather rectangular or stripe pattern.

Yet another finding is observed for a miscut along a perpendicular direction, as depicted in figure 3. Again, the $\sqrt{3}$ areas grow on the lower terrace side of step edges, i.e. towards [$\bar{1}$ 1 0], and with comparable rate at the IDBs. However, the growth at the IDBs proceeds mainly along the [1 1 $\bar{2}$] direction, whereas the growth towards the opposite direction, [$\bar{1}$ $\bar{1}$ 2], is almost completely suppressed. As a result, $\sqrt{3}$ patches form equilateral triangles at the IDBs, and right-angled triangles at the step edges. Consequently, the remaining patches of the 7 × 7 structure tend to resemble right-angled triangles, as can be seen from figure 3(b).

The LEEM images shown so far illustrate that the shape of the self-organized nanopattern can be chosen by the miscut orientation. For conditions close to thermal equilibrium, the structural size of the pattern is determined on the one hand by the width of the initial 7 × 7 domains on the terraces, which to some extent can be tuned e.g. by the cooling rate at the 1 × 1 to 7 × 7 phase transition, and on the other hand by the terrace length, which can be controlled via the miscut angle. In particular, for larger miscut angles in the range of a few tenths of a degree, our findings imply that pattern length scales below 100 nm can be achieved. Moreover, the choice of the deposition temperature would be less crucial in this case: the temperature has to be chosen

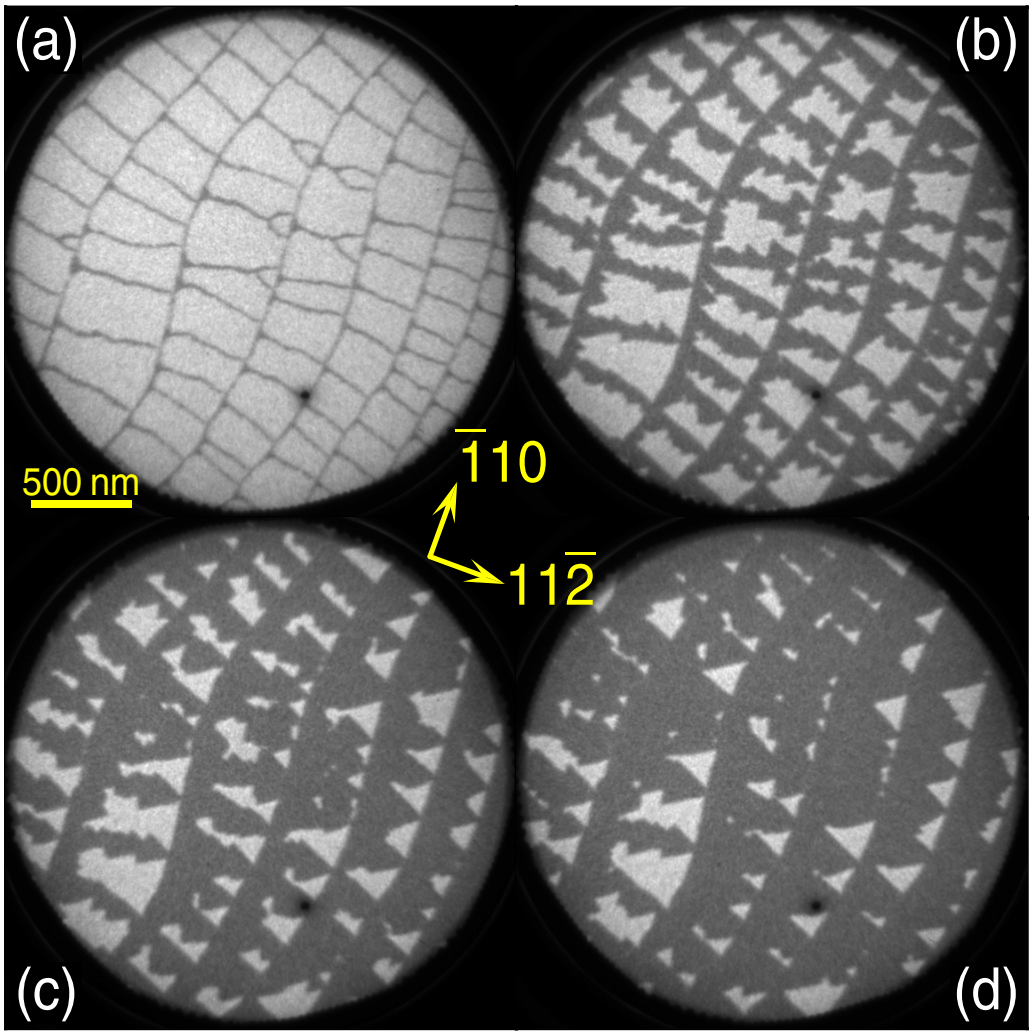

Figure 1. Bright-field LEEM images of Si(1 1 1) during Ga deposition at about 650 °C (field of view: 2.5 μm, $E = 3.5$ eV). Step edges run from bottom left to top right, the miscut (step-down) direction is towards [1 1 $\bar{2}$]. (a) Ga-terminated $\sqrt{3}$ domains (dark) nucleate at the initial domain boundaries (IDBs) of the 7×7 reconstruction (bright). From (a) to (d) the Ga coverage increases 0.06 ML (a), 0.19 ML (b), 0.26 ML (c) and 0.29 ML (d). $\sqrt{3}$ and remaining 7×7 domains are composed of equilateral triangles in a christmas-tree arrangement. See the movie.

such that homogeneous nucleation within the initial 7×7 domains is suppressed. Hence, for larger miscut angles, a wider temperature range could be used.

3.2. Scheme of $\sqrt{3}$ domain growth

In order to understand the dependence of the domain shape on the miscut orientation, it is worthwhile to consider the similarities in the findings for all different miscut orientations. Firstly, the domain boundaries between $\sqrt{3}$ and 7×7 always run along $\langle 1\,\bar{1}\,0 \rangle$, with the outward normal of the $\sqrt{3}$ pointing towards $\langle \bar{1}\,\bar{1}\,2 \rangle$. Secondly, the domain boundaries are very straight,

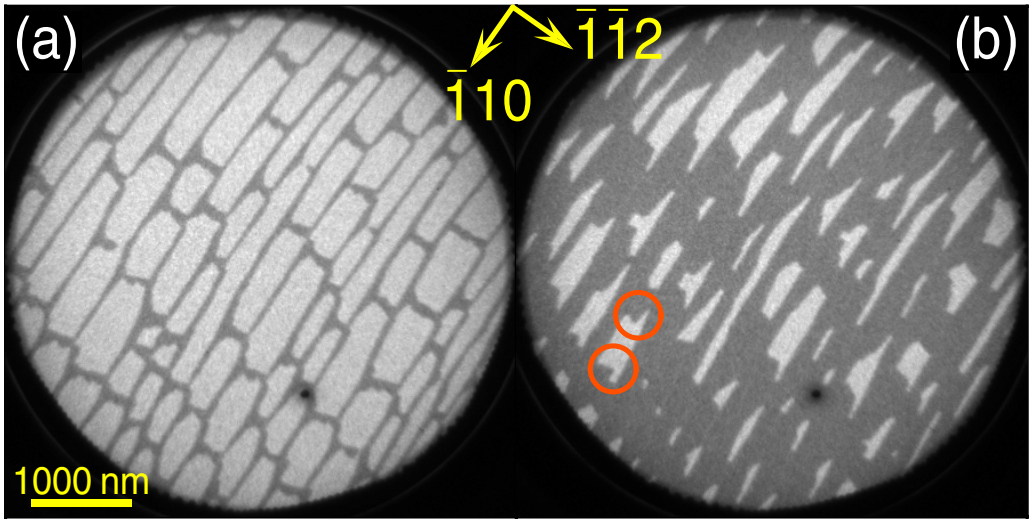

Figure 2. Bright-field LEEM images taken under similar conditions as in figure 1, but with miscut towards $[\bar{1}\,\bar{1}\,2]$. (Field of view: $5\,\mu$m, $E = 2.4$ eV.) The Ga coverage amounts to 0.09 ML (a), and 0.26 ML (b). The triangular nature of the $\sqrt{3}$ domain shape can still be seen, e.g. from the apexes in the red circles in (b). Overall, a rectangular pattern is formed. See the movie.

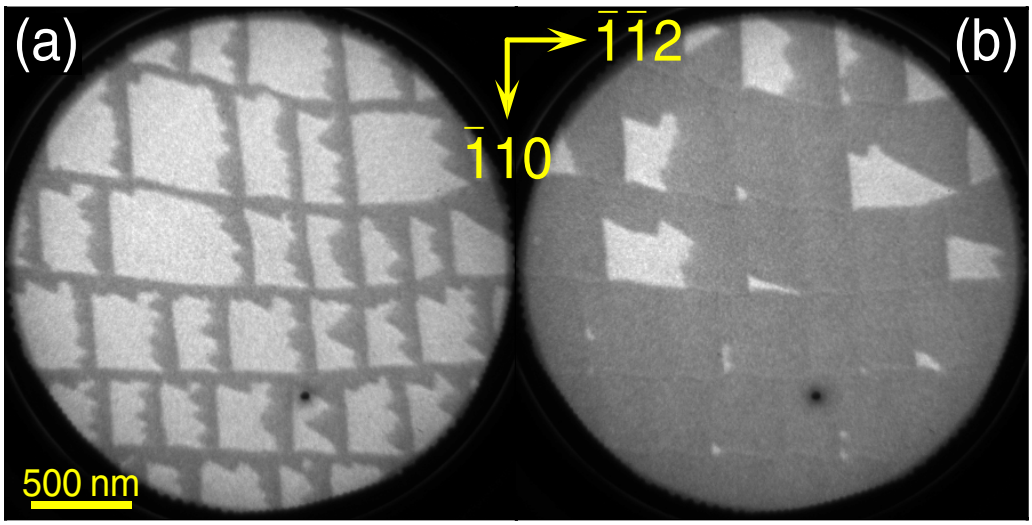

Figure 3. Bright-field LEEM images taken under similar conditions as in figures 1 and 2, but with miscut towards $[\bar{1}\,1\,0]$. (Field of view: $2.5\,\mu$m, $E = 3.5$ eV.) The Ga coverage amounts to 0.11 ML (a) and 0.29 ML (b). See the movie.

i.e. they do not exhibit many kinks. To a large extent, the kinks observed can be attributed to the coalescence of different $\sqrt{3}$ domains. Thirdly, the $\sqrt{3}$ structure always nucleates both at the lower terrace side of step edges as well as at IDBs, and step edges act as an efficient barrier for $\sqrt{3}$ growth.

From the observation that long straight domain boundaries between $\sqrt{3}$ and 7×7 domains are preferred over kinky short ones, it can be concluded that kink formation is energetically unfavourable. Starting with an ideal $\sqrt{3}$ domain with only straight domain boundaries, growth can only take place by kink formation, i.e. by single kink formation at defects like existing kinks (which are not available for an ideal $\sqrt{3}$ domain), step edges, or IDBs. The alternative mechanism, namely double kink formation at the straight edges is strongly suppressed, due to the large kink energy mentioned above. The $\sqrt{3}$ domain then grows while the single kink propagates, until it reaches an apex of the $\sqrt{3}$ domain; growth around such apexes is again suppressed, because it includes an intermediate double-kink-like stage. The injection of kinks from step edges and IDBs is also promoted by an increased local adsorbate concentration at these defects [11], which can as well be regarded to drive the initial nucleation of $\sqrt{3}$ domains.

Within this model, which is also sketched in figure 4, all the different growth speeds and domain shapes can be well explained.

An azimuthal orientation of the miscut along $[1\,1\,\bar{2}]$ (cf figure 1) leads to a $\sqrt{3}$ domain growth at the step edges as depicted in figure 4(a). This results in the formation of equilateral triangles at the step edges. It has to be kept in mind that the $\sqrt{3}$ domains grow towards the lower terrace only. In contrast, the $\sqrt{3}$ structure can grow towards both directions at the IDBs. Therefore, at the IDBs the domains grow as shown in figures 4(b) and (c). This allows for a symmetrical growth around the IDBs leading to the christmas-tree arrangement observed in figure 1.

For a miscut along $[\bar{1}\,\bar{1}\,2]$ (cf figure 2), a domain boundary segment parallel to the step edges will hardly move away from the step edge, since the only way to do so is via double kink formation (see figure 4(d')). Instead, a long stripe parallel to the step edge slowly evolves by repeated kink injection from the step edge, as shown in figure 4(d). At the IDBs, again figures 4(b) and (c) apply, which leads to an equal growth in the $[1\,\bar{1}\,0]$ and $[\bar{1}\,1\,0]$ directions.

If the miscut is perpendicular to $[\bar{1}\,\bar{1}\,2]$ (cf figure 3), the growth at the step edges proceeds as either sketched in figure 4(b) or figure 4(c). At the IDBs, figures 4(a) and (d) apply for growth towards $[1\,1\,\bar{2}]$ and $[\bar{1}\,\bar{1}\,2]$, respectively. Therefore, the growth at the IDBs cannot be symmetrical for such a miscut orientation. The domains hardly grow towards the $[\bar{1}\,\bar{1}\,2]$ direction and equilateral triangles are formed much faster on the $[1\,1\,\bar{2}]$ side.

3.3. Generalizing the growth scheme

3.3.1. Comparison to STM. The growth mechanism proposed here is based on generic properties of the surface system, i.e. the line and kink energies of the $\sqrt{3}$–7×7 domain boundary and their anisotropy. This explains why similar results are found for this system under quite different experimental conditions. Figure 5 shows a Si(1 1 1) surface with miscut along $[1\,1\,\bar{2}]$, monitored with STM during thermal annealing at about 400 °C, after room temperature deposition of less than 1/3 ML Ga. At this temperature, the magic clusters [12], which form at low temperature, become unstable and Ga renucleates in $\sqrt{3}$ domains, leaving patches of bare Si(1 1 1)-7×7 behind. Compared to these 7×7 areas, the $\sqrt{3}$ domains on each terrace appear slightly brighter for the imaging conditions chosen in figure 5. In agreement with the LEEM results (cf figure 1), both the $\sqrt{3}$ domains and remaining the 7×7 domains form equilateral triangles for this miscut orientation. Though the structures after room temperature deposition and annealing at 400 °C are smaller than those obtained after deposition at 650 °C, this clearly reveals that the surface topology is governed by energetics, not by surface kinetics.

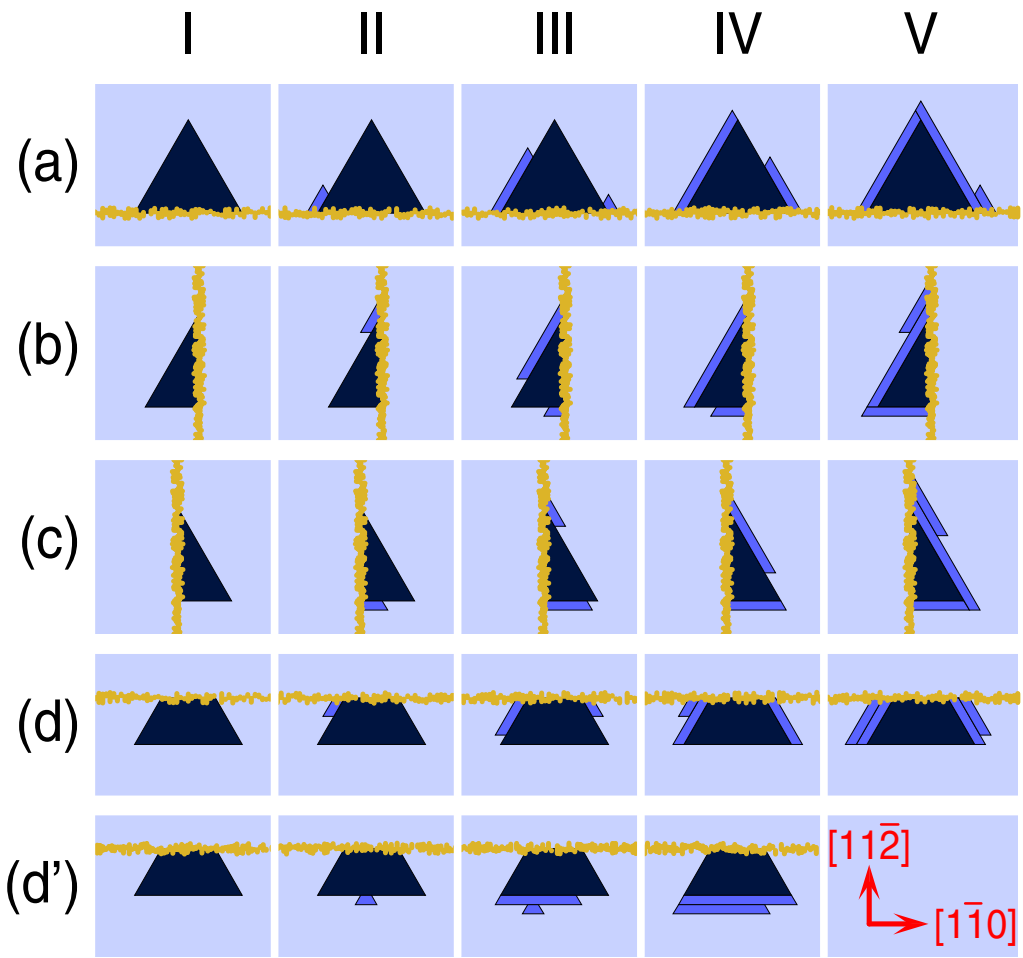

Figure 4. Sketch of a growth model showing subsequent stages (I–V) of the evolution of a $\sqrt{3}$ domain (dark), for different orientations (a)–(d) with respect to 1D defects (fuzzy yellowish lines), i.e. either step edges or IDBs. (I) Ideal $\sqrt{3}$ domain without kinks. (II) A single kink nucleates at the 1D defect, which then (III) propagates towards the apex while the next kink is injected. (IV) and (V): further evolution. In cases (a)–(c), the domain shape and aspect ratio is preserved, whereas for (d) a narrow stripe along the 1D defect evolves. The less probable case of double kink formation is shown in (d′).

From atomically resolved STM images (not shown), we find that the domain boundaries, which run along $\langle 1\,\bar{1}\,0\rangle$, are connecting the corner holes of the 7×7 reconstruction, and that the faulted halves of the 7×7 unit meshes are directly attached to the domain boundary. This leaves the energetically favourable DAS structure [13] of the adjacent 7×7 unit cells virtually unchanged and might explain the preferential orientation of the domain boundaries along $\langle 1\,\bar{1}\,0\rangle$. These findings are in agreement with a previous STM study [8], in which the authors investigated the phase transition from $\sqrt{3}$ to 7×7 by thermal desorption after room temperature deposition of more than 1/3 ML Ga. The authors also observed either a stripe-like or a triangular pattern, depending on miscut orientation. Hence, the growth behaviour we found for the $\sqrt{3}$ domains is not only virtually independent of surface kinetics, but it is also reversible.

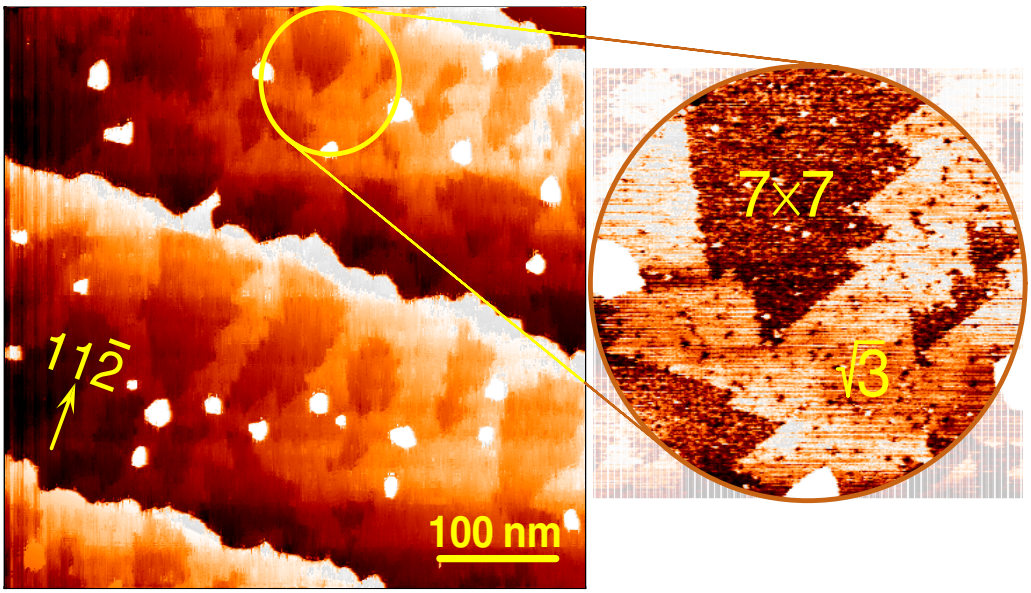

Figure 5. Empty-state STM images ($U = -1\,\mathrm{V}$, $I = 0.3\,\mathrm{nA}$) of Ga/Si(1 1 1) after room temperature deposition of 0.24 ML Ga, taken during annealing at 400 °C. The miscut is along [1 1 $\bar{2}$]. On each terrace, $\sqrt{3}$ domains appear slightly brighter than 7 × 7 domains. Both domain types form equilateral triangles. The very bright areas are islands of bilayer height, with $\sqrt{3}$ structure.

3.3.2. Comparison to the Si(1 1 1) 1 × 1 to 7 × 7 phase transition. An even more general scheme of the pattern formation is obtained when comparing the results shown so far to LEEM images obtained during the phase transition of the bare substrate from 1 × 1 to 7 × 7 at 830 °C, such as the one shown in figure 6. Here, 7 × 7 domains nucleate at the upper terrace side of the step edges [14] (i.e. the 1 × 1 reconstruction remains at the lower terrace side), forming either stripes or triangles, depending on the orientation of the meandering step edges. The domain boundaries are very straight and run along ⟨1 $\bar{1}$ 0⟩ directions. The outward normal orientation of the 7 × 7 domains is identical to the one observed during the 7 × 7 to $\sqrt{3}$ transition.

All these similarities indicate that the interactions between 7 × 7 and 1 × 1 domains on one hand, and 7 × 7 and $\sqrt{3}$ domains on the other hand, are comparable. As an important interaction between the different phases, surface stress has to be considered [15]. With respect to the 7 × 7 reconstruction, both the Ga/Si-$\sqrt{3}$ as well as the Si-1 × 1 reconstruction impose less tensile surface stress. For Ga/Si-$\sqrt{3}$, this stress relief has been reported to amount to 80 meV Å^{-2} [16], and corresponding values for Si-1 × 1 range from 30 to 60 meV Å^{-2} [17, 18].

Regarding the kink energies and the anisotropy of the line energies, the local atomic arrangement at the domain boundaries is essential. From this point of view, it is noteworthy that the arrangement of the silicon atoms within the $\sqrt{3}$ and the 1 × 1 reconstruction is very similar. In this respect, the $\sqrt{3}$ structure with Ga on T_4 sites [19, 20] can be regarded as a 'distorted bulk-terminated structure'. Since this allows for similar atomic arrangements at the domain boundaries, our findings are explained in terms of generic properties of the Si(1 1 1) surface, namely the high kink energies and anisotropy of the 1 × 1–7 × 7 domain boundaries,

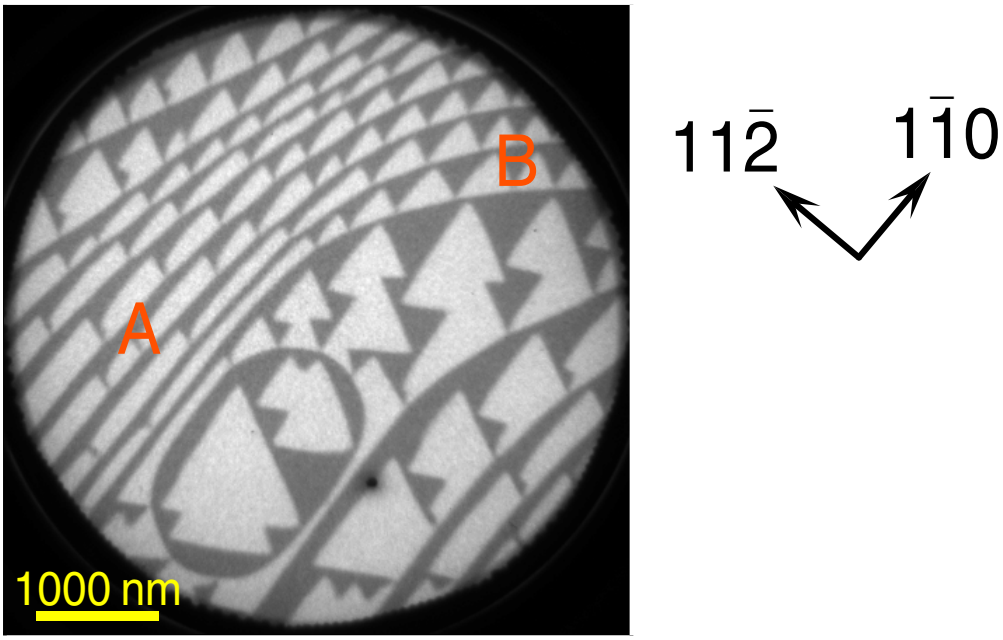

Figure 6. Bright-field LEEM image obtained during the 1×1 to 7×7 phase transition of the bare Si(1 1 1) substrate at ≈830 °C. (Field of view: 5 μm, $E = 12.1$ eV.) 1×1 domains appear dark, 7×7 domains appear bright and are attached to the upper terrace side of the step edges [14]. Depending on the step-edge orientation, either a stripe-like (region A) or a triangular (region B) domain shape is found.

which are preserved after Ga adsorption. Following this scheme, the formation of nanopatterns, like the ones observed here, could as well be expected for similar adsorbate structures, as long as the adsorbate-induced distortion of the bulk-terminated structure does not lead to too strong tensile surface stress.

3.4. Testing the scheme: In/Si(1 1 1)-$\sqrt{3} \times \sqrt{3}$-R 30°

In order to verify the scheme described above, we also performed similar adsorption experiments using indium instead of gallium. Typical results are shown in figure 7. As with Ga, high temperature low coverage adsorption of In leads to the formation of a $\sqrt{3} \times \sqrt{3}$-R 30° reconstruction [21]. Obviously, the nucleation and growth behaviour of this In/Si(1 1 1)-$\sqrt{3}$ structure is equivalent to Ga/Si(1 1 1)-$\sqrt{3}$. In the sample area depicted in figure 7, different orientations of the step edges are found simultaneously. In striking agreement with Ga, the shape of the nanopattern formed by In adsorption depends on this orientation. It is remarkable that the average local In coverage at the stripe-pattern (see area 'A' in figure 7(b)) is much lower than at the triangular pattern regions (e.g. area 'B' in the same image). On one hand, this reflects the different growth velocities mentioned above, on the other hand this concentration gradient clearly shows that the adsorbate mobility is high enough to allow diffusion in the micrometre range. This can be regarded as a further important prerequisite for the presently observed pattern formation.

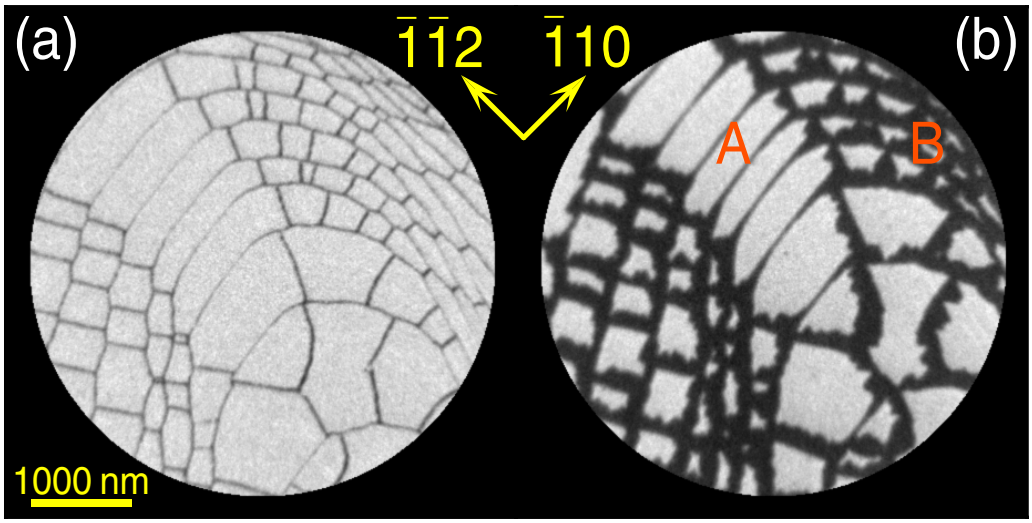

Figure 7. Bright-field LEEM images of Si(1 1 1) during indium deposition at about 450 °C. (Field of view: 5 μm, $E = 11.1$ eV.) (a) In/Si(1 1 1)-$\sqrt{3}$ domains (dark) nucleate at step edges and domain boundaries of the 7 × 7 reconstruction. The In coverage amounts to 0.05 ML. (b) After further In deposition (0.16 ML coverage), different pattern shapes evolve for different step-edge orientations (compare the regions labelled as A and B). See the movie.

4. Summary

In conclusion, we have shown that a Ga/Si(1 1 1) surface nanopattern can be achieved, the shape of which can be tuned by an adequate surface miscut orientation. This allows for a further degree of freedom for subsequent processing, e.g. for the growth of Ge 3D nanostructures [7]. The pattern formation is based on heterogeneous nucleation at domain boundaries of the initial 7 × 7 reconstruction and at step edges. Therefore, the size of the nanopattern can be tuned by the absolute value of the miscut angle. Provided that the adsorbate surface diffusion is sufficient, and provided that the adsorbate-induced surface reconstruction does not impose too strong tensile surface stress, our proposed model for the underlying mechanism of pattern formation predicts that other adsorbates on Si(1 1 1) could exhibit a similar behaviour. This prediction has been confirmed replacing Ga with In, supporting the validity of the model.

Acknowledgments

We would like to acknowledge Wacker Siltronic for kind supply of highly oriented Si wafers. This work has been supported by the European Community—Research Infrastructure Action under the FP6 (contract no. RII3–CT–2004–506008), and by the Deutsche Forschungsgemeinschaft (grant no. FA 363/6).

References

[1] Lyo I W and Avouris P 1991 *Science* **253** 173
[2] Eigler D M and Schweizer E K 1990 *Nature* **344** 524
[3] Dagata J A, Schneir J, Harary H H, Evans J, Postek M T and Bennett J 1990 *Appl. Phys. Lett.* **56** 2001
[4] Lyding J W, Shen T C, Hubacek J S, Tucker J R and Abein G C 1994 *Appl. Phys. Lett.* **64** 2010
[5] Men F K, Liu F, Wang P J, Chen C H, Cheng D L, Lin J L and Himpsel F J 2002 *Phys. Rev. Lett.* **88** 096105
[6] Fölsch S, Helms A, Riemann A, Repp J, Meyer G and Rieder K H 2002 *Surf. Sci.* **497** 113
[7] Schmidt Th, Flege J I, Gangopadhyay S, Clausen T, Falta J, Locatelli A and Heun S 2005 *Phys. Rev. Lett.* submitted
[8] Fujita K, Kusumi Y and Ichikawa M 1996 *Appl. Phys. Lett.* **68** 631
[9] Schmidt T, Heun S, Slezak J, Diaz J and Prince K 1998 *Surf. Rev. Lett.* **5** 1287
[10] Locatelli A, Bianco A, Cocco D, Cherifi S, Heun S, Marsi M, Pasqualetto M and Bauer E 2003 *J. Physique IV (France)* **104** 99
[11] Gangopadhyay S, Schmidt Th and Falta J 2004 *Surf. Sci.* **552** 63
[12] Lai M Y and Wang Y L 2001 *Phys. Rev.* B **64** 241404 (R)
[13] Takayanagi K, Tanishiro Y, Takahashi M and Takahashi S 1985 *J. Vac. Sci. Technol.* A **3** 1502
[14] Telieps W and Bauer E 1985 *Surf. Sci.* **162** 163
[15] Hannon J B, Meyer zu Heringdorf F J, Tersoff J and Tromp R M 2001 *Phys. Rev. Lett.* **86** 4871
[16] Martinez R E, Augustyniak W M and Golovchenko J A 1990 *Phys. Rev. Lett.* **64** 1035
[17] Twesten R D and Gibson J M 1994 *Phys. Rev.* B **50** 17628
[18] Hannon J B and Tromp R M 2001 *J. Vac. Sci. Technol.* A **19** 2596
[19] Kawazu A and Sakama H 1988 *Phys. Rev.* B **37** 2704
[20] Patel J R, Zegenhagen J, Freeland P E, Hybertsen M S, Golovchenko J A and Chen D M 1989 *J. Vac. Sci. Technol.* B **7** 894
[21] Kraft J, Ramsey M G and Netzer F P 1997 *Phys. Rev.* B **55** 5384